Matter and Radiation at Extremes

RESEARCH ARTICLE | SEPTEMBER 11 2024

Exotic compounds of monovalent calcium synthesized at high pressure

Jun Kong ; Kaiyuan Shi ; Artem R. Oganov ; Jiaqing Zhang; Lei Su ; Xiao Dong

Matter Radiat. Extremes 9, 067803 (2024)
https://doi.org/10.1063/5.0222230

Matter and Radiation at Extremes

RESEARCH ARTICLE

pubs.aip.org/aip/mre

Exotic compounds of monovalent calcium synthesized at high pressure

Cite as: Matter Radiat. Extremes 9, 067803 (2024); doi: 10.1063/5.0222230
Submitted: 6 June 2024 • Accepted: 13 August 2024 •
Published Online: 11 September 2024

Jun Kong,[1,2] Kaiyuan Shi,[2] Artem R. Oganov,[3] Jiaqing Zhang,[2] Lei Su,[2,4,a)] and Xiao Dong[1,a)]

AFFILIATIONS

[1] Key Laboratory of Weak-Light Nonlinear Photonics and School of Physics, Nankai University, Tianjin 300071, China
[2] Center for High Pressure Science and Technology Advanced Research, Beijing 100093, China
[3] Skolkovo Institute of Science and Technology, Skolkovo Innovation Center, Bolshoy Boulevard 30, Building 1, Moscow 121205, Russia
[4] Key Laboratory of Photochemistry, Institute of Chemistry, University of Chinese Academy of Sciences, Chinese Academy of Sciences, Beijing 100190, China

[a)] **Authors to whom correspondence should be addressed:** leisu2050@iccas.ac.cn and xiao.dong@nankai.edu.cn

ABSTRACT

It is well known that atoms of the same element in different valence states show very different chemical behaviors. Calcium is a typical divalent metal, sharing or losing both of its valence electrons when forming compounds. Attempts have been made to synthesize compounds of monovalent calcium ions for decades, but with very little success (e.g., in clusters). Pressure can result in substantial changes in the properties of atoms and chemical bonding, creating an extensive variety of unique materials with special valence states. In this study, using the *ab initio* evolutionary algorithm USPEX, we search for stable calcium–chlorine (Ca–Cl) system compounds at pressures up to 100 GPa. Besides the expected compound $CaCl_2$, we predict three new compounds with monovalent Ca to be stable at high pressures, namely, CaCl, Ca_5Cl_6, and Ca_3Cl_4. According to our calculations, CaCl is stable at pressures above 18 GPa and is predicted to undergo a transition from nonmagnetic *Fm*-3*m*-CaCl to ferromagnetic *Pm*-3*m*-CaCl at 40 GPa. Ca_5Cl_6 and Ca_3Cl_4 are stable at pressures above 37 and 73 GPa, with space groups *P*-1 and *R*-3, respectively. Following these predictions, we successfully synthesized *Pm*-3*m*-CaCl in laser-heated diamond anvil cell experiments. The emergence of the unusual valence state at high pressures reveals exciting opportunities for creating entirely new materials in sufficiently large quantities for a variety of potential applications.

I. INTRODUCTION

Calcium (Ca) is a very abundant element in the Universe and a crucial component of many important materials, e.g., animal bones, signaling molecules in cells, and fluorite.[1–3] Like other Group II alkaline-earth elements, calcium has a silvery metallic appearance in its pure form, but is not found in this condition in nature because of its high reactivity. Again like other alkaline earth metal atoms, calcium atoms have very low electronegativity and easily lose two valence electrons when bonded to other elements. This corresponds to valence II or oxidation state +2, which is perfectly consistent with the octet rule. Can one imagine a situation in which a calcium atom gives away only one of its valence electrons, i.e., is monovalent? Stable compounds with low-valence calcium have long been sought.[4] For instance, low-valence calcium has been explored in clusters, such as $LCa(N_2)CaL$ (where L is a bulky β-diketiminate ligand), which can be characterized crystallographically.[5] Two-dimensional CaCl crystals with monovalent calcium ions have been synthesized on reduced graphene oxide (rGO) membranes, revealing many interesting properties.[6] The atomic valence is the number of electrons that an atom gives or takes in the process of chemical bonding. It substantially affects the physical and chemical properties of compounds—in particular, their color, stability, electrical conductivity, and redox properties. Among the many examples are the oxides of chromium, including the black semiconducting chromium(II) oxide CrO with strongly reducing properties, the green insulating Cr_2O_3 with Cr(III), the half-metallic CrO_2 with Cr(IV), and the red insulating CrO_3 with Cr(VI) and strong oxidizing properties. In contrast to most transition metal atoms, calcium has long been assumed to always be in a divalent state, Ca(II), in its compounds. The discovery of compounds with low-valence calcium will not only improve our knowledge of chemical laws, but should

also be valuable for the facilitation of unconventional chemical reactions and the synthesis and exploration of exotic materials and their properties (e.g., for catalysis, ferromagnetism, and hydrogen storage). For example, variable valence of calcium could lead to new catalysts, and if the remaining electron is localized, the monovalent calcium atom Ca(I) will be magnetic.[6]

Unexpected stoichiometries can be synthesized under extreme conditions (high pressures and temperatures). Recently, pressure–composition phase diagrams have been predicted for many binary systems, including Na–Cl, Ca–C, Na–He, Zn–N, Ti–O, Ta–N, S–O, Rb–B, Fe–He, Ce–N, Fe–Bi, Fe–F, and others,[7–18] and these theoretical predictions have provided the basis for the successful experimental synthesis of previously unexpected compounds such as Na_3Cl, Ca_2C_3, and Na_2He under high pressures. Such exotic compounds may exhibit unusual electronic, magnetic, optical, and mechanical properties due to their unusual electronic distributions and peculiar bonding,[19] for example, the best known high-temperature superconductors belonging to this class of exotic high-pressure compounds, including LaH_{10}, YH_6, ThH_{10}, H_3S, BaH_{12}, and Sr(Hf, Zr)H_{18}.[20–25]

In the present work, systematic searches for stable compounds in the calcium–chlorine system are carried out at pressures of up to 100 GPa using the *ab initio* evolutionary algorithm USPEX.[26–28] Besides the anticipated calcium(II) compound $CaCl_2$, we find three new compounds, CaCl, Ca_5Cl_6, and Ca_3Cl_4, which are predicted to be stable at high pressures according to our calculations. CaCl is stable at pressures above 18 GPa with monovalent Ca cations. It is predicted to undergo a phase transition from *Fm*-3*m*-CaCl to *Pm*-3*m*-CaCl at 40 GPa. Ca_5Cl_6 is stable above 37 GPa with space group *P*-1. Ca_3Cl_4 is stable above 73 GPa with space group *R*-3. We also analyze the band structures, densities of states (DOS), electron localization functions (ELFs),[29] and many other properties of these compounds, which exhibit many interesting characteristics. Following our predictions, we successfully synthesize *Pm*-3*m*-CaCl in laser-heated diamond anvil cell (DAC) experiments. Our results indicate that the emergence of an unexpected valence state at high pressure has great potential for creating entirely new materials.

II. METHODS

A. Computational details

Stable stoichiometries and crystal structures were predicted using USPEX[26–28] in combination with the Vienna *Ab initio* Simulation Package (VASP) code[30] within the framework of density functional theory (DFT) and the generalized gradient approximation (GGA), using the exchange–correlation functional of Perdew, Burke, and Ernzerhof (PBE).[31] We employed the projector-augmented wave method[32] with $3s^2 3p^6 4s^2$ and $3s^2 3p^5$ electrons treated as the valence electrons for Ca and Cl atoms, respectively.

In these calculations, all stoichiometries were allowed, with the only constraint being that randomly produced structures contained no more than 50 atoms in the primitive cell. The initial population of 120 structures and 20 compositions evolved toward the fittest states (with the fitness being calculated as the vertical distance of each candidate solution from the thermodynamic convex hull), and new structures/compositions were produced from the fittest individuals of the previous generation automatically using heredity, transmutation, and softmutation. Furthermore, randomly produced structures were added to each generation using symmetric[28] and topological[33] random structure generators.

Our searches proceeded in two steps. First, we performed full searches in the Ca–Cl system and found that $CaCl_2$ is a stable compound at all pressures studied here. We then performed searches on the calcium-rich side, i.e., for the Ca–$CaCl_2$ system. The enthalpy of formation per atom of Ca_nCl_m is defined as

$$\Delta H(\mathrm{Ca}_n\mathrm{Cl}_m) = \left[H(\mathrm{Ca}_n\mathrm{Cl}_m) - \left(n - \frac{m}{2}\right)H(\mathrm{Ca}) - \left(\frac{m}{2}\right)H(\mathrm{CaCl}_2)\right]/(m+n),$$

where all enthalpies H are given at the same pressure and zero temperature. At a given pressure, compounds located on the convex hull are thermodynamically stable rather than decomposing into any isochemical mixture of compounds, while the compounds located above the convex hull are metastable or unstable.

The most interesting structures were further relaxed using the VASP code at high pressures, and their properties were calculated to higher precision with a basis set cutoff of 800 eV and a uniform *k*-point grid with *k*-point spacing below $2\pi \times 0.02$ Å^{-1}. The energy differences, stress tensors, and structural parameters showed excellent convergence in our calculations. We computed the phonon spectra of all the predicted stable structures using the PHONOPY code to check their dynamical stability.[34] We used VASP and the PBE functional to determine the band structures and DOS of these compounds. Bader analysis was performed to explore chemical bonding and analyze the charge transfer.[35] The VASPKIT code was used to post-process of the data produced by the VASP code.[36] Crystal orbital Hamilton population (COHP) analysis was performed using LOBSTER.[37] Crystal structures were visualized using VESTA.[38]

B. Experimental

High-purity $CaCl_2$ (Alfa Aesar, ultradry, 99.99%) powder and a calcium plate (Alfa Aesar, 99.5%) were loaded into a DAC with culets of 200 μm inside an inert Ar glovebox. The sample chamber was a 100 μm-diameter hole drilled in a pre-indented rhenium gasket using a drilling system at the Center for High Pressure Science and Technology Advanced Research (HPSTAR). The calcium plate in the sample chamber was surrounded by $CaCl_2$ powder positioned on the diamond anvil. The samples were compressed to 50 GPa and then heated to about 2000 K for 3–5 min over the entire sample by a laser-heating (1064 nm) system at HPSTAR. Double-sided laser heating was used to apply sufficient heating to the samples. During laser heating, the temperatures of the samples were calculated by collecting the emitted thermal radiation, correcting for the optical system response, and fitting the spectral data to the Wien function. The pressure was calibrated from the fluorescence of ruby balls placed inside the sample chamber.[39]

After laser heating, the X-ray diffraction (XRD) data for samples at different pressures (20–60 GPa) were collected. Synchrotron XRD data were collected on the synchrotron beamlines 4W2 at the Beijing Synchrotron Radiation Facility and BL15U1 at the Shanghai

Synchrotron Radiation Facility (λ = 0.6199 Å). The XRD patterns were integrated using Dioptas,[40] and full profile refinements were performed using FullProf.[41]

III. RESULTS AND DISCUSSION

We explored the pressure–composition phase diagram of the Ca–$CaCl_2$ system at pressures of 0, 30, 60, and 100 GPa. By evaluating the enthalpy of formation ΔH for each composition at different pressures, the convex hulls for the Ca–$CaCl_2$ system at different pressures were constructed and are shown in Fig. 1(a). We then carried out more careful calculations of the enthalpy under different pressures for the stable structures on the convex hulls, which enabled us to construct the pressure–composition diagram of the Ca–$CaCl_2$ system [Fig. 1(b)].

Elemental Ca is predicted to undergo several phase transitions induced by pressure: fcc-bcc-$I4_1/amd$-$P4_32_12$. In our calculations, under ambient conditions, Ca adopts the fcc structure, while bcc-Ca is stable from 7.5 to 33 GPa, followed by transitions to $I4_1/amd$ and $P4_32_12$ at 33 and 78 GPa, respectively. These results agree with those of previous studies.[42–45] Furthermore, the pressure–composition phase diagram predicted by our calculations contains a surprisingly large number of new stable compounds. The phase diagram shows that $CaCl_2$ remains stable over the whole pressure range investigated here (0–100 GPa), and many new compounds become stable at elevated pressures. We found that CaCl, Ca_5Cl_6, and Ca_3Cl_4 are thermodynamically stable at high pressures [Fig. 1(b)], and are all located on the convex hull from 18, 37, and 73 GPa, respectively, to at least 100 GPa. Calculations reveal that Ca, $CaCl_2$, and CaCl undergo structural phase transitions at high pressures. The crystallographic parameters of all stable phases are listed in Table S1 (supplementary material), and crystal structures are shown in Fig. 2. Lattice dynamics calculations suggest that all the phases shown in the phase diagram [Fig. 1(b)] have no phonons with imaginary frequencies (i.e., are dynamically stable) in their predicted pressure ranges of thermodynamic stability (Fig. S1, supplementary material). To investigate the electronic properties of these compounds, we calculated their ELFs, electronic band structures, Bader charges, integrated crystal orbital Hamiltonian populations (ICOHPs), and DOS. As shown in Fig. S2 (supplementary material), the electronic DOS shows that all these new compounds (CaCl, Ca_5Cl_6, and Ca_3Cl_4) are metallic.

$CaCl_2$ is the only known thermodynamically stable compound in the Ca–Cl system. From standard chemical considerations such as the octet rule, $CaCl_2$ is the only expected compound of calcium and chlorine. $CaCl_2$ has been studied at high pressures, and experiments have found that within a narrow pressure range of 0–10 GPa, it crystallizes in five different phases with the $CaCl_2$, α-PbO_2, EuI_2, SrI_2, and $PbCl_2$ (cotunnite) structure types, with the $PbCl_2$-type structure being stable up to at least 25 GPa.[46] In our calculations, $CaCl_2$ is a stable stoichiometry in the entire region of explored pressures, and we find a new post-cotunnite P-62m structure [Fig. 2(a)] to be stable in the 18–82 GPa pressure range. Figure S3(a) (supplementary material) shows the band structure and the projected density of states (PDOS) of P-62m-$CaCl_2$. It has a direct DFT bandgap of 2.71 eV, in contrast to the zero-pressure structure of $Pnnm$-$CaCl_2$, which has a direct DFT bandgap of 5.34 eV. The DOS near the Fermi level is dominated by the p electronic states of chlorine. Interestingly, above 82 GPa, P-62m-$CaCl_2$ transforms back into the cotunnite structure, which remains stable up to at least 100 GPa.

From our calculations, a new weakly metallic compound, CaCl, becomes stable at 18 GPa. It has two stable phases, which have a rocksalt (or B1) structure (space group Fm-3m) and a CsCl-type (or B2) structure (space group Pm-3m), as shown in Figs. 2(b) and 2(c). The phase transition from the rock salt to the CsCl-type structure, accompanied by an increase in the coordination number from 6 to 8, is commonly observed at high pressures.[7] For CaCl, B1–CaCl is stable at pressures from 18 to 40 GPa, while B2–CaCl is stable over a wide range of pressures from 40 GPa to at least 100 GPa. Phonon calculations show that the dynamical stability of B1–CaCl is retained as the pressure decreases to 10 GPa and it is not quenchable to ambient pressure, but B2–CaCl retains its dynamical stability when quenched to 0 GPa, which indicates that once formed at high pressure, this phase might be quenchable to ambient pressure.

To determine the valence of Ca in CaCl, we computed the Bader charges of the Ca and Cl atoms (Table S1, supplementary

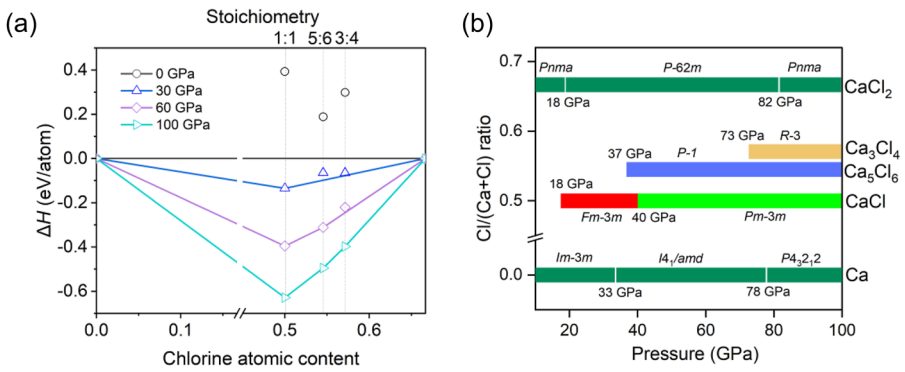

FIG. 1. (a) A convex hull diagram for the Ca–$CaCl_2$ system at selected pressures. At a given pressure, the compounds located on the convex hull are thermodynamically stable. ΔH denotes the enthalpy of formation per atom. (b) Pressure–composition phase diagram of the Ca–$CaCl_2$ system.

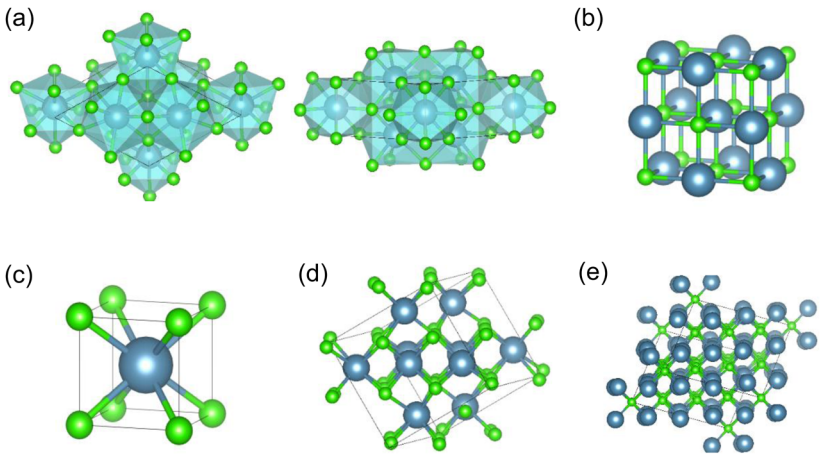

FIG. 2. Crystal structures of stable Ca–Cl compounds. (a) *P*-62*m*-$CaCl_2$ at 60 GPa along the (001) and (110) directions. (b) *Fm*-3*m*-CaCl at 30 GPa. (c) *Pm*-3*m*-CaCl at 50 GPa. (d) *P*-1-Ca_5Cl_6 at 50 GPa. (e) *R*-3-Ca_3Cl_4 at 80 GPa. The large blue and small green spheres represent Ca and Cl atoms, respectively.

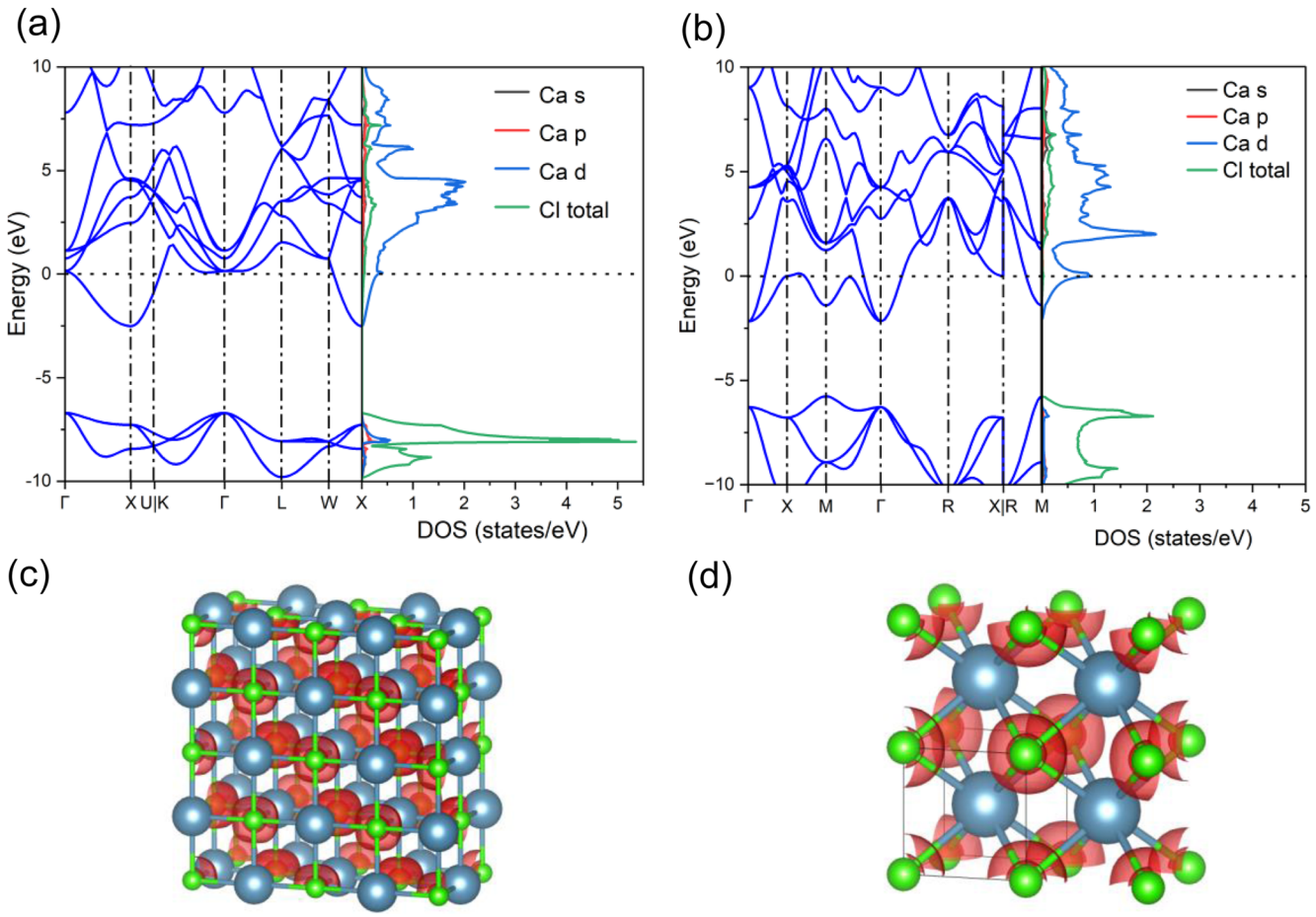

FIG. 3. Electronic structures of *Fm*-3*m*-CaCl at 30 GPa and *Pm*-3*m*-CaCl at 50 GPa. (a) Band structure and projected density of states (PDOS) of *Fm*-3*m*-CaCl at 30 GPa. (b) Band structure and PDOS of *Pm*-3*m*-CaCl at 50 GPa. (c) ELF of *Fm*-3*m*-CaCl at 30 GPa. The ELF = 0.8 isosurface is shown. (d) ELF of *Pm*-3*m*-CaCl at 50 GPa (showing the ELF = 0.6 isosurface). The large blue and small green spheres represent Ca and Cl atoms, respectively.

material). To interpret these values, we recall that in all cases known so far, Bader charges have smaller absolute values than the corresponding chemical valences. For example, Bader charges of 1.3–1.4 on Ca atoms in $CaCl_2$ are compatible with the classical divalent state, whereas the charge of 0.9 in *Pm*-3*m*-CaCl can be interpreted as evidence of the Ca(I) state. The intermediate charge of 1.1 in *Fm*-3*m*-CaCl is possibly a sign of the mixed-valence state. These unusual valence states are expected to carry many new properties. As previous studies have indicated, the pressure-induced change of orbital energies leads to occupation of orbitals with a higher angular momentum at high pressures.[47,48] As the Ca atom is compressed, the occupation of 3*d* orbitals increases at the expense of 4*s* orbitals, and this $4s \rightarrow 3d$ electron transfer in calcium under pressure makes calcium an "incipient transition metal." The pressure-driven *s*–*d* transfer enables monovalent calcium to exist and stabilizes these new compounds. This is proven by the electronic band structure and PDOS, which indicate that the metallicity of CaCl phases is predominantly due to the 3*d* electrons of calcium [Figs. 3(a) and 3(b)]. In forming CaCl, a calcium atom gives one electron to chlorine, while the second valence electron of the Ca atom can either remain on the atomic *d* orbital of calcium (in this case, calcium is monovalent, giving $Ca^{+}Cl^{-}$) or delocalize over the whole crystal as an electron gas (in this case, the valence of calcium is two). Below, we argue that in CaCl, we have a mixture of these two situations, but with an essential contribution from the monovalent configuration.

The ELF provides additional information on the electronic properties of CaCl. As shown in Figs. 3(c) and 3(d), the valence ELFs of *Fm*-3*m*-CaCl and *Pm*-3*m*-CaCl are mainly concentrated on chlorine atoms. Further insight is provided by ICOHP values, which are negative for bonding interactions, and we see significant Ca–Cl and Ca–Ca bonding in both modifications of CaCl (Table S2, supplementary material). Both the metallicity and the presence of Ca–Ca bonding indicate some activity of the second valence electron of calcium (and hence a contribution of the divalent state). There is also a significant degree of localization of that electron, conferring new properties to the compound (i.e., the essential contribution of the monovalent state). As discussed above, CaCl undergoes a phase transition from a rock salt to a CsCl-type structure at 40 GPa. Interestingly, this phase transition is accompanied by a transition from a Pauli paramagnet to a ferromagnet. Usually, increasing pressure leads to a suppression of magnetism, because atoms in the high-spin state have larger radii than in low-spin states. The opposite, however, can also occur—for example, potassium has been predicted to produce *s*-band ferromagnetism under pressure.[49] Here, ferromagnetism comes from the second valence electron of Ca localized on the *d* orbital. However, the magnetic moment of *Pm*-3*m*-CaCl decreases with pressure from 0.25 μB per Ca atom at 40 GPa to 0.04 μB per Ca atom at 100 GPa and eventually collapses at 110 GPa (Fig. 4).

From our calculations, as pressure increases, the atomic volumes of Ca and Cl become similar, making a Ca → Cl substitution possible. This indeed happens and makes Ca_5Cl_6 and Ca_3Cl_4 thermodynamically stable. Ca_5Cl_6 is a low-symmetry (space group *P*-1) phase, thermodynamically stable from 37 GPa to at least 100 GPa. It has only one ground-state structure under the whole pressure range explored here. Its crystal structure can be obtained from that of a *Pm*-3*m*-CaCl crystal by replacing Ca atoms with Cl at some sites [Fig. 2(d)]. The Bader charges of Cl atoms occupying the Ca position are smaller ($-0.7|e|$) than those of other Cl atoms ($-1|e|$). The other stable compound, Ca_3Cl_4, is predicted to have a space group *R*-3 and is thermodynamically stable at pressures ranging from 73 GPa to at least 100 GPa. Its crystal structure can also be obtained from that of a *Pm*-3*m*-CaCl crystal just like Ca_5Cl_6 [Fig. 2(e)]. To further investigate the properties of Ca_5Cl_6 and Ca_3Cl_4, we analyzed their electronic structures. As expected, both Ca_3Cl_4 and Ca_5Cl_6 are metallic, and their DOS at the Fermi level come mainly from Ca 3*d* electrons, similar to CaCl [Figs. S3(c) and S3(e), supplementary material]. Figures S3(d) and S3(f) show the similarity of the ELF distributions of Ca_3Cl_4 and Ca_5Cl_6 to that of CaCl, whose valence electrons are mainly concentrated around the Cl atoms.

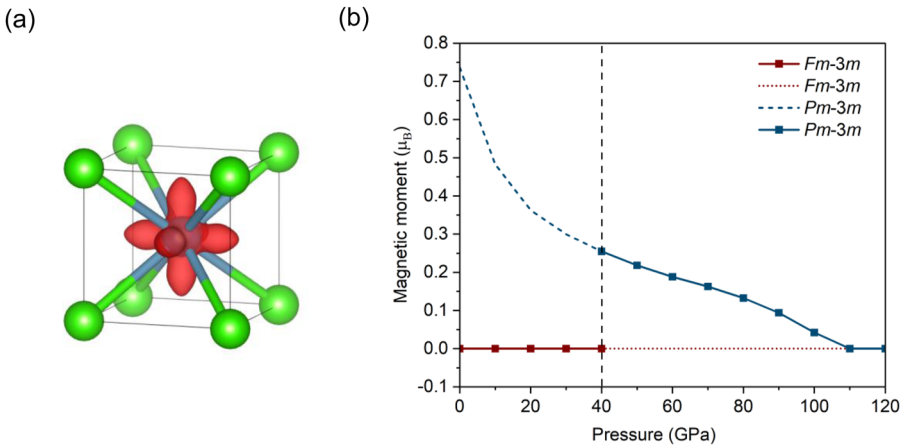

FIG. 4. Ferromagnetism of *Pm*-3*m*-CaCl under high pressure. (a) Spin density at 50 GPa. The 0.0035 *e*/bohr^3 isosurface is shown. The blue and green spheres represent Ca and Cl atoms, respectively. (b) Magnetic moment per formula unit as a function of pressure. The increasing delocalization of the *d* electrons of calcium leads to magnetic collapse at 110 GPa.

Having understood these compounds theoretically, we decided to experimentally verify their stability. We performed high-pressure experiments on the Ca–Cl system in a laser-heated DAC to validate our predictions. A Ca plate and $CaCl_2$ powder were loaded into a Re gasket hole of the DAC, then compressed gradually to 50 GPa, and then laser-heated to a temperature of about 2000 K. A minute change in pressure in the sample chamber before and after the laser-heating process was observed and was probably caused by changes in sample volume due to chemical reaction. At this pressure, the formation of *Pm*-3*m*-CaCl is expected on the basis of its thermodynamic stability [Fig. 1(a)].

Powder XRD patterns changed greatly after laser heating. Figure 5(a) shows powder XRD data obtained at 50 GPa after laser heating. There is a good match between the experimental data and simulated diffraction patterns. Most of the reflections do indeed correspond to the predicted *P*-62*m*-$CaCl_2$ and *Pm*-3*m*-CaCl, and the most obvious peak of *Pm*-3*m*-CaCl belongs to (110) [Fig. 5(a)]. Minor differences between calculated and experimental XRD

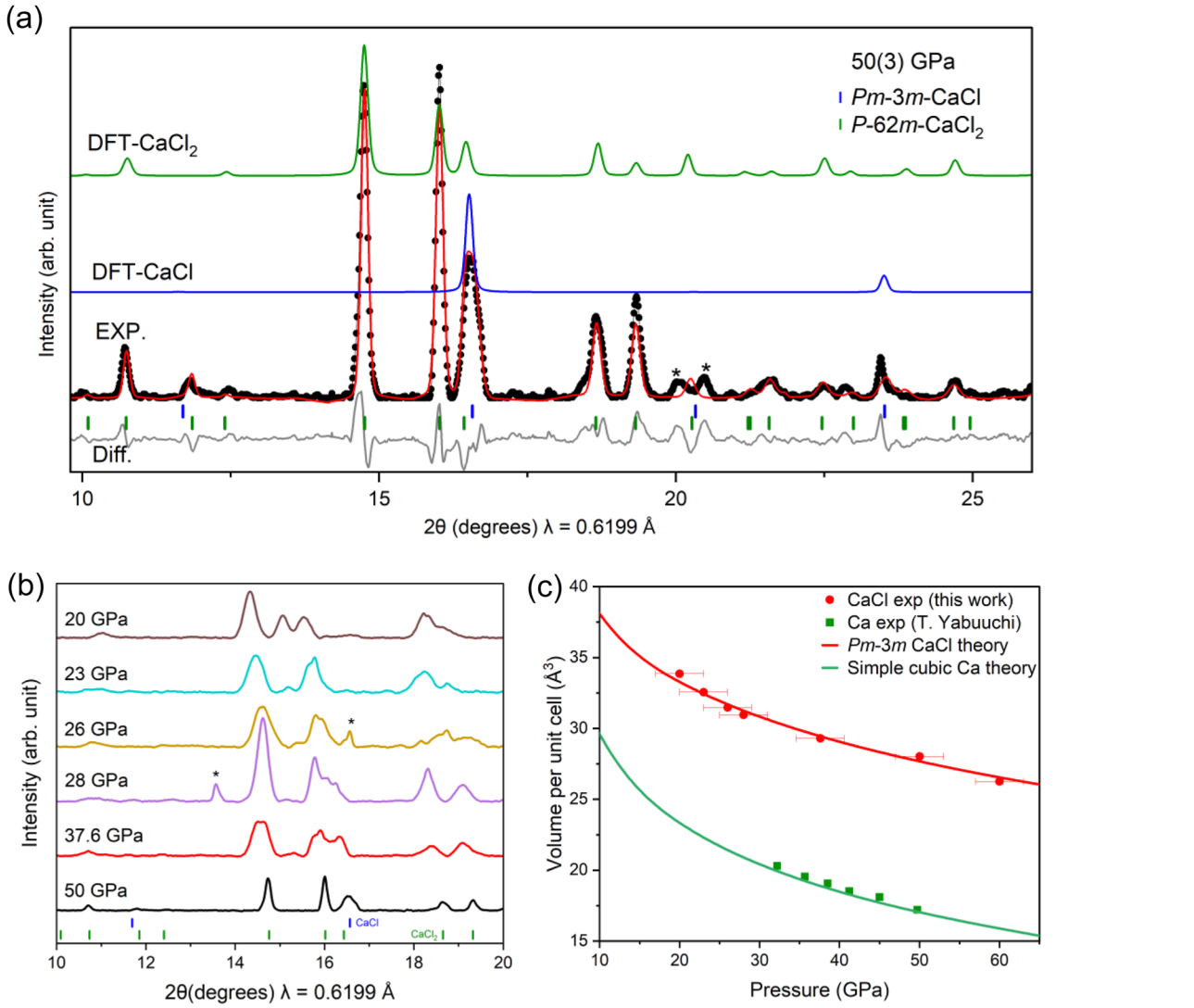

FIG. 5. Powder XRD patterns and equation of state. (a) *Pm*-3*m*-CaCl and *P*-62*m*-$CaCl_2$ synthesized at 50(3) GPa. The X-ray wavelength is 0.6199 Å. Experimental data (black points) are compared with simulated patterns with DFT (blue and green lines) and full-profile refinements using the Rietveld method (red line) with differences. Some peaks marked by asterisks may belong to impurities. The positions of reflections of *Pm*-3*m*-CaCl and *P*-62*m*-$CaCl_2$ are indicated by blue and green tick marks, respectively. (b) Powder XRD patterns of *Pm*-3*m*-CaCl and *P*-62*m*-$CaCl_2$ at different pressures. Some peaks marked by asterisks may belong to impurities. (c) Equation of state of CaCl synthesized in DAC in comparison with that of Ca.[50] Experimental parameters (symbols) are compared with DFT predictions (lines). The error bars correspond to the experimental pressure uncertainty due to pressure gradients and pressure measurements.[39]

patterns are likely due mostly to impurities and anisotropic broadening of diffraction peaks, probably caused by inhomogeneous elastic stresses, which always arise under high pressures during laser heating. It is worth noting that some of the new diffraction rings are spotty (Fig. S4, supplementary material), indicating that we do not have a perfect powder with a very large number of randomly oriented crystallites. This texture is due to the heating and cooling process of the samples. Importantly, we did not observe elemental calcium in the products, which means that the elemental calcium had completely reacted.

On changing the pressure on the sample, we found that *Pm*-3*m*-CaCl was stable upon quenching down to at least 20 GPa. Additionally, some small peaks, marked with asterisks in Fig. 5(b), were observed during decompression, and these might be contributed by some minority impurities at different sampling positions. The peak position (2θ) of (110) of *Pm*-3*m*-CaCl moved from 16.59° at 50 GPa to 15.57° at 20 GPa, which means that the lattice parameter changed from 3.04 to 3.24 Å. After quenching of the sample to ambient pressure and exposing it to air, we could not observe any peaks related to the products, which means that these were unstable at ambient pressure and temperature. From the XRD data, we obtained the pressure–volume equation of state of *Pm*-3*m*-CaCl in the pressure range 20–60 GPa [Fig. 5(c)]. There was a good agreement between the experimental and theoretical equations of state of *Pm*-3*m*-CaCl. The experimental *P*–*V* data were fitted to a second-order Birch–Murnaghan equation of state with B_0 = 42.68 GPa, while B_0 was 44.29 GPa from theoretical predictions. To further exclude the possible presence of unreacted elemental calcium influencing the observation of *Pm*-3*m*-CaCl diffraction peaks, we compare the cell volumes of *Pm*-3*m*-CaCl and simple cubic Ca in Fig. 5(c). We can see that the volume differences between the two at the same pressures are sufficiently large to completely rule out the presence of elemental calcium in the sample. The fact that the reaction Ca + $CaCl_2$ = 2CaCl producing CaCl took place only after laser heating implies a considerable activation barrier for this reaction.

IV. CONCLUSION

In summary, we have studied the Ca–Cl system using state-of-the-art theoretical predictions and experimental high-pressure synthesis. We have produced a pressure–composition phase diagram for this system at pressures of up to 100 GPa and synthesized a new anomalous compound, calcium monochloride (CaCl), containing calcium in a unique monovalent state, Ca(I), as predicted by theory. CaCl is predicted to undergo a pressure-induced transition from a nonmagnetic NaCl-type phase to a ferromagnetic CsCl-type phase at 40 GPa. Ca_5Cl_6 and Ca_3Cl_4 are stable at pressures above 37 and 73 GPa with space groups *P*-1 and *R*-3, respectively. The predicted *Pm*-3*m*-CaCl was synthesized in a laser-heated DAC at 50 GPa and shown to be quenchable down to at least 20 GPa. The application of pressure enables the creation of a wider palette of valence states of atoms, greatly increasing the range of accessible properties. For example, making calcium a variable-valence element could lead to completely unexpected calcium-based catalysts. This new side of the seemingly simple chemistry of calcium may provide important surprises in geochemistry and planetary sciences, since calcium is one of the most abundant planet-forming elements, and high pressures are typical of planetary interiors. Even under ambient conditions, the Ca(I) state may be more accessible than commonly thought (in intermediate states of chemical reactions, for example). Upon rigorous theoretical and experimental analysis, what was initially thought to be a fundamentally simple chemical system has revealed itself to be a tremendously rich system with novel physics and chemistry. This work demonstrates that by revisiting simple systems, it is possible to develop new chemical principles and identify remarkable new materials and phenomena.

SUPPLEMENTARY MATERIAL

See the supplementary material for the crystal structure and Bader charges of stable Ca–Cl compounds (Table S1), calculated ICOHPs for Ca–Ca, Ca–Cl, and Cl–Cl pairs in CaCl (Table S2), phonon dispersion curves of *Fm*-3*m*-CaCl, *Pm*-3*m*-CaCl, Ca_5Cl_6, and Ca_3Cl_4 (Fig. S1), electronic DOS of calcium chlorides (Fig. S2), electronic structures of Ca_5Cl_6 at 40 GPa, Ca_3Cl_4 at 80 GPa, and $CaCl_2$ at 60 GPa (Fig. S3), and a two-dimensional image of the XRD pattern after laser heating (Fig. S4).

ACKNOWLEDGMENTS

This work was supported by the National Science Foundation of China (Grant Nos. 92263101, 12174200, 21627802, 51722209, and 21273206), the Science Challenge Project (Grant No. TZ2016001), the Key Research Project of Higher Education (Grant Nos. 15A140016 and 2010GGJS-110), and the National Key R&D Program of China (Grant No. YS2018YFA070119). The work of A.R.O. was supported by the Russian Science Foundation (Grant No. 24-43-00162). The calculations were performed and supported by Tianhe II in Guangzhou and the Supercomputing Center of Nankai University (NKSC).

AUTHOR DECLARATIONS

Conflict of Interest

The authors have no conflicts to disclose.

Author Contributions

X.D. designed the research. X.D. and J.K. performed and analyzed the calculations. L.S. designed experiments. J.K. and K.S performed the experiment. L.S., X.D., J.K., and J.Z. analyzed the experimental data. All authors contributed to the interpretation and discussion of the data. J.K., X.D., A.R.O., and L.S. wrote the manuscript.

Jun Kong: Data curation (equal); Formal analysis (equal); Investigation (equal); Resources (equal); Validation (equal); Writing – original draft (equal); Writing – review & editing (equal). **Kaiyuan Shi**: Data curation (equal); Formal analysis (equal); Investigation (equal). **Artem R. Oganov**: Conceptualization (equal); Data curation (equal); Funding acquisition (equal); Methodology (equal). **Jiaqing Zhang**: Data curation (equal); Formal analysis (equal);

Investigation (equal). **Lei Su**: Data curation (equal); Formal analysis (equal); Funding acquisition (equal); Methodology (equal); Project administration (equal); Resources (equal); Supervision (equal); Writing – original draft (equal); Writing – review & editing (equal). **Xiao Dong**: Conceptualization (equal); Data curation (equal); Formal analysis (equal); Funding acquisition (equal); Methodology (equal); Project administration (equal); Software (equal); Supervision (equal); Validation (equal); Visualization (equal); Writing – original draft (equal); Writing – review & editing (equal).

DATA AVAILABILITY

The data that support the findings of this study are available from the corresponding authors upon reasonable request.

REFERENCES

[1] M. J. Berridge, M. D. Bootman, and P. Lipp, "Calcium—A life and death signal," Nature **395**(6703), 645–648 (1998).

[2] D. Gebauer, A. Völkel, and H. Cölfen, "Stable prenucleation calcium carbonate clusters," Science **322**(5909), 1819–1822 (2008).

[3] C. Cazorla and D. Errandonea, "Superionicity and polymorphism in calcium fluoride at high Pressure," Phys. Rev. Lett. **113**(23), 235902 (2014).

[4] C. Jones, "Open questions in low oxidation state group 2 chemistry," Commun. Chem. **3**(1), 159–164 (2020).

[5] B. Rösch, T. Gentner, J. Langer, C. Färber, J. Eyselein, L. Zhao, C. Ding, G. Frenking, and S. Harder, "Dinitrogen complexation and reduction at low-valent calcium," Science **371**(6534), 1125–1128 (2021).

[6] L. Zhang, G. Shi, B. Peng, P. Gao, L. Chen, N. Zhong, L. Mu, L. Zhang, P. Zhang, L. Gou, Y. Zhao, S. Liang, J. Jiang, Z. Zhang, H. Ren, X. Lei, R. Yi, Y. Qiu, Y. Zhang, X. Liu, M. Wu, L. Yan, C. Duan, S. Zhang, and H. Fang, "Novel 2D CaCl crystals with metallicity, room-temperature ferromagnetism, heterojunction, piezoelectricity-like property and monovalent calcium ions," Natl. Sci. Rev. **8**(7), nwaa274 (2020).

[7] W. Zhang, A. R. Oganov, A. F. Goncharov, Q. Zhu, S. E. Boulfelfel, A. O. Lyakhov, E. Stavrou, M. Somayazulu, V. B. Prakapenka, and Z. Konôpková, "Unexpected stable stoichiometries of sodium chlorides," Science **342**(6165), 1502–1505 (2013).

[8] .Y.-L. Li, S.-N. Wang, A. R. Oganov, H. Gou, J. S. Smith, and T. A. Strobel, "Investigation of exotic stable calcium carbides using theory and experiment," Nat. Commun. **6**(1), 6974 (2015).

[9] X. Dong, A. R. Oganov, A. F. Goncharov, E. Stavrou, S. Lobanov, G. Saleh, G.-R. Qian, Q. Zhu, C. Gatti, V. L. Deringer, R. Dronskowski, X.-F. Zhou, V. B. Prakapenka, Z. Konôpková, I. A. Popov, A. I. Boldyrev, and H.-T. Wang, "A stable compound of helium and sodium at high pressure," Nat. Chem. **9**(5), 440–445 (2017).

[10] X. Shi, Z. Yao, and B. Liu, "New high pressure phases of the Zn–N system," J. Phys. Chem. C **124**(7), 4044–4049 (2020).

[11] K. Li, J. Wang, and A. R. Oganov, "High-pressure phase diagram of the Ti–O system," J. Phys. Chem. Lett. **12**(23), 5486–5493 (2021).

[12] M. Bykov, E. Bykova, A. V. Ponomareva, I. A. Abrikosov, S. Chariton, V. B. Prakapenka, M. F. Mahmood, L. Dubrovinsky, and A. F. Goncharov, "Stabilization of polynitrogen anions in tantalum–nitrogen compounds at high pressure," Angew. Chem., Int. Ed. **60**(16), 9003–9008 (2021).

[13] W. Lu, S. Liu, G. Liu, K. Hao, M. Zhou, P. Gao, H. Wang, J. Lv, H. Gou, G. Yang, Y. Wang, and Y. Ma, "Disproportionation of SO_2 at high pressure and temperature," Phys. Rev. Lett. **128**(10), 106001 (2022).

[14] P. Zhang, Y. Tian, Y. Yang, H. Liu, and G. Liu, "Stable Rb–B compounds under high pressure," Phys. Rev. Res. **5**(1), 013130 (2023).

[15] B. Monserrat, M. Martinez-Canales, R. J. Needs, and C. J. Pickard, "Helium-Iron compounds at terapascal pressures," Phys. Rev. Lett. **121**(1), 015301 (2018).

[16] C. Ding, J. Yuan, X. Wang, T. Huang, Y. Wang, and J. Sun, "Single-bonded nitrogen chain and porous nitrogen layer via Ce–N compounds," Mater. Adv. **4**(9), 2162–2173 (2023).

[17] M. Amsler, S. S. Naghavi, and C. Wolverton, "Prediction of superconducting iron–bismuth intermetallic compounds at high pressure," Chem. Sci. **8**(3), 2226–2234 (2017).

[18] W. Lu, S. Liu, M. Zhou, H. Wang, G. Liu, H. Liu, and Y. Ma, "Observation of iron with eight coordination in iron trifluoride under high pressure," Angew. Chem., Int. Ed. **63**(16), e202319320 (2024).

[19] G. Shi, L. Chen, Y. Yang, D. Li, Z. Qian, S. Liang, L. Yan, L. H. Li, M. Wu, and H. Fang, "Two-dimensional Na–Cl crystals of unconventional stoichiometries on graphene surface from dilute solution at ambient conditions," Nat. Chem. **10**(7), 776–779 (2018).

[20] M. Somayazulu, M. Ahart, A. K. Mishra, Z. M. Geballe, M. Baldini, Y. Meng, V. V. Struzhkin, and R. J. Hemley, "Evidence for superconductivity above 260 K in lanthanum superhydride at megabar pressures," Phys. Rev. Lett. **122**(2), 027001 (2019).

[21] I. A. Troyan, D. V. Semenok, A. G. Kvashnin, A. V. Sadakov, O. A. Sobolevskiy, V. M. Pudalov, A. G. Ivanova, V. B. Prakapenka, E. Greenberg, A. G. Gavriliuk, I. S. Lyubutin, V. V. Struzhkin, A. Bergara, I. Errea, R. Bianco, M. Calandra, F. Mauri, L. Monacelli, R. Akashi, and A. R. Oganov, "Anomalous high-temperature superconductivity in YH6," Adv. Mater. **33**(15), 2006832 (2021).

[22] D. V. Semenok, A. G. Kvashnin, A. G. Ivanova, V. Svitlyk, V. Y. Fominski, A. V. Sadakov, O. A. Sobolevskiy, V. M. Pudalov, I. A. Troyan, and A. R. Oganov, Superconductivity at 161 K in thorium hydride ThH_{10}: Synthesis and properties. Mater. Today **33**, 36–44 (2020).

[23] S. Mozaffari, D. Sun, V. S. Minkov, A. P. Drozdov, D. Knyazev, J. B. Betts, M. Einaga, K. Shimizu, M. I. Eremets, L. Balicas, and F. F. Balakirev, "Superconducting phase diagram of H_3S under high magnetic fields," Nat. Commun. **10**(1), 2522 (2019).

[24] W. Chen, D. V. Semenok, A. G. Kvashnin, X. Huang, I. A. Kruglov, M. Galasso, H. Song, D. Duan, A. F. Goncharov, V. B. Prakapenka, A. R. Oganov, and T. Cui, "Synthesis of molecular metallic barium superhydride: Pseudocubic BaH_{12}," Nat. Commun. **12**(1), 273 (2021).

[25] C. Deng, M. Wang, H. Huang, M. Xu, W. Zhao, M. Du, H. Song, and T. Cui, "High-T_c superconductors in the ternary Sr-Hf/Zr-H system at high pressure," Phys. Rev. B **109**(18), 184516 (2024).

[26] A. R. Oganov and C. W. Glass, "Crystal structure prediction using ab initio evolutionary techniques: Principles and applications," J. Chem. Phys. **124**(24), 244704 (2006).

[27] A. R. Oganov, A. O. Lyakhov, and M. Valle, "How evolutionary crystal structure prediction works—And why," Acc. Chem. Res. **44**(3), 227–237 (2011).

[28] A. O. Lyakhov, A. R. Oganov, H. T. Stokes, and Q. Zhu, "New developments in evolutionary structure prediction algorithm USPEX," Comput. Phys. Commun. **184**(4), 1172–1182 (2013).

[29] A. D. Becke and K. E. Edgecombe, "A simple measure of electron localization in atomic and molecular systems," J. Chem. Phys. **92**(9), 5397–5403 (1990).

[30] J. Hafner, "Materials simulations using VASP—A quantum perspective to materials science," Comput. Phys. Commun. **177**(1–2), 6–13 (2007).

[31] J. P. Perdew, K. Burke, and M. Ernzerhof, "Generalized gradient approximation made simple," Phys. Rev. Lett. **77**(18), 3865 (1996).

[32] P. E. Blöchl, "Projector augmented-wave method," Phys. Rev. B **50**(24), 17953 (1994).

[33] P. V. Bushlanov, V. A. Blatov, and A. R. Oganov, "Topology-based crystal structure generator," Comput. Phys. Commun. **236**, 1–7 (2019).

[34] A. Togo and I. Tanaka, "First principles phonon calculations in materials science," Scr. Mater. **108**, 1–5 (2015).

[35] G. Henkelman, A. Arnaldsson, and H. Jónsson, "A fast and robust algorithm for Bader decomposition of charge density," Comput. Mater. Sci. **36**(3), 354–360 (2006).

[36] V. Wang, N. Xu, J.-C. Liu, G. Tang, and W.-T. Geng, "VASPKIT: A user-friendly interface facilitating high-throughput computing and analysis using VASP code," Comput. Phys. Commun. **267**(2021), 108033 (2021).

[37] R. Nelson, C. Ertural, J. George, V. L. Deringer, G. Hautier, and R. Dronskowski, "LOBSTER: Local orbital projections, atomic charges, and chemical-bonding

analysis from projector-augmented-wave-based density-functional theory," J. Comput. Chem. **41**(21), 1931–1940 (2020).
[38]K. Momma and F. Izumi, "*VESTA3* for three-dimensional visualization of crystal, volumetric and morphology data," J. Appl. Crystallogr. **44**(6), 1272–1276 (2011).
[39]H. Mao, J.-A. Xu, and P. Bell, "Calibration of the ruby pressure gauge to 800 kbar under quasi-hydrostatic conditions," J. Geophys. Res.: Solid Earth **91**(B5), 4673–4676, https://doi.org/10.1029/jb091ib05p04673 (1986).
[40]C. Prescher and V. B. Prakapenka, "*DIOPTAS*: A program for reduction of two-dimensional X-ray diffraction data and data exploration," High Pressure Res. **35**(3), 223–230 (2015).
[41]J. Rodríguez-Carvajal, "Recent advances in magnetic structure determination by neutron powder diffraction," Physica B **192**(1–2), 55–69 (1993).
[42]A. R. Oganov, Y. Ma, Y. Xu, I. Errea, A. Bergara, and A. O. Lyakhov, "Exotic behavior and crystal structures of calcium under pressure," Proc. Natl. Acad. Sci. U. S. A. **107**(17), 7646–7651 (2010).
[43]Y. Yao, D. D. Klug, J. Sun, and R. Martoňák, "Structural prediction and phase transformation mechanisms in calcium at high pressure," Phys. Rev. Lett. **103**(5), 055503 (2009).
[44]T. Ishikawa, H. Nagara, N. Suzuki, J. Tsuchiya, and T. Tsuchiya, "Review of high pressure phases of calcium by first-principles calculations," J. Phys. Conf. Ser. **215**(1), 012105 (2010).
[45]T. Ishikawa, H. Nagara, N. Suzuki, T. Tsuchiya, and J. Tsuchiya, "High-pressure phases of calcium: Prediction of phase VI and upper-pressure phases from first principles," Phys. Rev. B **81**(9), 092104 (2010).
[46]J.-M. Léger, J. Haines, and C. Danneels, "Phase transition sequence induced by high-pressure in $CaCl_2$," J. Phys. Chem. Solids **59**(8), 1199–1204 (1998).
[47]X. Dong, A. R. Oganov, H. Cui, X.-F. Zhou, and H.-T. Wang, "Electronegativity and chemical hardness of elements under pressure," Proc. Natl. Acad. Sci. U. S. A. **119**(10), e2117416119 (2022).
[48]J. P. Connerade, V. K. Dolmatov, and P. A. Lakshmi, "The filling of shells in compressed atoms," J. Phys. B: At. Mol. Opt. Phys. **33**(2), 251–264 (2000).
[49]C. J. Pickard and R. J. Needs, "Predicted pressure-induced *s*-band ferromagnetism in alkali metals," Phys. Rev. Lett. **107**(8), 087201 (2011).
[50]T. Yabuuchi, Y. Nakamoto, K. Shimizu, and T. Kikegawa, "New high-pressure phase of calcium," J. Phys. Soc. Jpn. **74**(9), 2391–2392 (2005).